5-4-2023

Quantifying and Comparing Water Transit Time Distributions in Urban Beaver and Stormwater Retention Ponds in the Atlanta, GA Metropolitan Area

Claire Wadler

Follow this and additional works at: https://scholarworks.gsu.edu/geosciences_theses

Quantifying and Comparing Water Transit Time Distributions in Urban Beaver and Stormwater

Retention Ponds in the Atlanta, GA Metropolitan Area

by

Claire Wadler

Under the Direction of Sarah Ledford, PhD and Luke Pangle, PhD

A Thesis Submitted in Partial Fulfillment of the Requirements for the Degree of

Master of Science

in the College of Arts and Sciences

Georgia State University

2023

ABSTRACT

Best management practices, including stormwater ponds, are implemented to mitigate the effects of urban stormwater. While these structures may effectively modulate local surface runoff, empirical analyses suggest their cumulative effect on watershed-scale streamflow is marginal. Beaver impoundments, by altering the downstream hydrologic flow regime, may offer a natural, complementary means of managing stormwater. This study seeks to determine how the transit times of water traversing urban beaver ponds compares to those occurring within stormwater ponds, by adding a conservative tracer (Br⁻) near-instantaneously at inflow points to three beaver impoundments and two stormwater ponds in Atlanta, GA in dry (fall) and wet (spring) seasonal conditions. The expected difference in flow due to seasonal conditions was not observed at all sites. Transit times were longer in the stormwater ponds than the beaver ponds in both seasons, and both pond types show altered flow path configurations due to short term weather dynamics.

INDEX WORDS: Beaver dams, Stormwater retention ponds, Conservative tracer tests, Transit times, Water storage, Flow attenuation

Quantifying and Comparing Water Transit Time Distributions in Urban Beaver and Stormwater

Retention Ponds in the Atlanta, GA Metropolitan Area

by

Claire Wadler

Committee Chairs: Sarah H. Ledford

Luke A. Pangle

Committee: Nadine Kabengi

Electronic Version Approved:

Office of Graduate Services

College of Arts and Sciences

Georgia State University

May 2023

DEDICATION

This thesis would not have been possible without the love and support of my parents and sister. To the friends I have made here in Atlanta who helped me feel at home in a new city mid-pandemic, and to my cat who kept me company every late night working on this endeavor.

ACKNOWLEDGEMENTS

TABLE OF CONTENTS

LIST OF TABLES

LIST OF FIGURES

LIST OF ABBREVIATIONS

BDA: Beaver Dam Analog

BMP: Best Management Practices

Br^-: Bromide

BTC: Breakthrough Curve

LID: Low Impact Development

MTT: Mean Transit Time

NaBr: Sodium Bromide

SWMP: Stormwater Management Pond

RTD: Residence Time Distribution

TTD: Transit Time Distribution

1   INTRODUCTION

1.1   Stressors of Urban Streams and Mitigation Efforts

Runoff from impervious surfaces alters stream hydrology, morphology, and water quality in urban areas. The 'Urban Stream Syndrome' (Walsh et al., 2005) synthesizes the common problems urban streams face, which includes a flashier hydrograph, where there is a decrease in the lag time between precipitation events and peak streamflow, and increases in stormflow magnitude. The presence of impervious surfaces and the direct routing of runoff into streams also inhibits infiltration of precipitation into soils, which can reduce groundwater recharge and baseflow in streams (Diem et al., 2018; O'Driscoll et al., 2010). Reduced baseflow, however is not common to all urban streams, as leaky infrastructure and pre-urbanization conditions can also impact, and sometimes enhance, baseflow (Bhaskar et al., 2016). Channel incision and widening from altered drainage networks can occur, increasing sediment loads and adversely affecting water quality (Paul and Meyer, 2001). The water quality of urban streams is then further degraded by increased nutrient loads from aging infrastructure and legacy land use (Paul and Meyer, 2001; Kaushal and Belt., 2012). The nutrient loading that occurs in headwater streams can cause environmental degradation in downstream coastal systems as the headwater streams become a source of contaminant transport (O'Driscoll et al., 2010; Walsh et al., 2005).

Widespread adoption of Best Management Practices (BMPs) began in the 1990s to help mitigate the impacts of increasing urbanization on streams (Environmental Protection Agency, 2009). These practices include stormwater management ponds (SWMPs), which are designed to hold a portion of stormwater runoff to promote infiltration or release it at a gradual rate while maintaining a certain level of water between storm events. By retaining water, these BMPs can

provide a greater degree of pollutant removal through gravity settling, infiltration, and microbial and vegetation nutrient removal (Strassler et al., 1999).

Optimizing the design of the ponds (i.e., the shape, size, and depth), as well as the residence time of the water flowing through these systems is important for effectively controlling stormflows and alleviating downstream water quality issues, but lack of continuing maintenance, short-circuiting within the ponds, and increasing development pressures can hinder the performance of BMPs (Beckingham et al., 2019; Mallin et al., 2002). Within the Piedmont physiographic region, the expansion of urban areas is expected to further stress stream ecosystems (Terando et al., 2014; Van Metre et al., 2019), and land acquisition and maintenance costs can cause BMPs to become quite expensive (Weiss et al., 2007). Other methods of managing stormwater, such as Low Impact Development (LID), have gained popularity, and recent literature has highlighted the advantages of incorporating more nature-based solutions into stormwater management while tailoring stormwater management practices to individual cases (Golden and Hoghooghi, 2018; Miles and Band, 2015).

1.2   Effect of Beaver Impoundments on Flow and Chemistry of Streams

As beaver populations rebound across North America, following their near extirpation in the 1800s, there is interest in exploring the ability of beaver impoundments to function as a natural stormwater management method (Bailey et al., 2019). Beaver are considered both a keystone species and ecosystem engineers due to their dam building activity. In landscapes with marginal human impacts, the often dense network of dams beaver construct can inundate upstream floodplains and create wetlands that provide habitat for other species to live, while also increasing the upstream flow path complexity and decreasing longitudinal connectivity (Puttock et al., 2017; Wegener et al., 2017). Established beaver dams can reduce peak flows, total

stormflow, and stream flashiness due to their storage capacity for water (Puttock et al., 2021), though this ability varies depending on the intensity of the storm event (Neumayer et al., 2020; Westbrook et al., 2020).

The increased flow path complexity both at the surface and subsurface associated with beaver dams may help improve water quality. By increasing the flow path complexity and decreasing the local water velocities, beaver impoundments may promote longer residence times of water (Puttock et al., 2017; Puttock et al., 2021; Brazier et al., 2020). Given long enough residence times, the chance of biogeochemical reactions that can remove pollutants, such as denitrification, occurring increases (Zarnetske et al., 2011). In watersheds with high nitrate loading, beaver ponds promote nitrate removal through denitrification processes (Lazar et al., 2015). In another study, it was found that while beaver ponds can extend the lateral extent of the hyporheic zone by altering subsurface flow paths, there was a lack of associated biogeochemical transformation (Wang et al., 2018). The enhanced flow path served as a net source for DOC and nitrogen, potentially due to the flow paths not being long enough to reach the net sink threshold. Wegener et al. (2017) observed variable source-sink dynamics of beaver impoundments, finding that nutrients were retained in high flow conditions due to greater lateral connectivity, and released during low flow conditions. The delivery of nutrients and organic material during higher flows, and then the increased residence times experienced in lower flows promote metabolic processing rates. The ability for beaver impoundments to improve water quality therefore seems to vary based on upstream lateral connectivity and availability of limiting reagents.

Investigations into a beaver dam complex's ability to improve water quality, attenuate flow, and restore streams to their natural floodplains in agriculture and forest dominated catchments are numerous, but the impact of beaver impoundments within urban stream networks

is less understood. Geomorphic features and the availability of building material are important controls for how complex the beaver sequences can become (Naiman et al., 1988; Puttock et al., 2020). This complexity, including dam size, density, and configuration, has been shown to be important to the beaver impoundments' ability to alter hydrologic flow regimes, and may be limited by the topographic and habitat conditions in heavily urbanized areas. The potential for beaver-human conflict also exists, as the constructed ponds can encroach upon and cause damage to private land and infrastructure, and beaver are often viewed as a nuisance species (Bailey et al., 2019). Parts of the urban landscape may be amenable to beaver, though, and their impoundments may have positive impacts on the flow, morphology, water quality, and species diversity within urban streams, both locally and downstream.

1.3   Quantifying Transit Time Distributions through Tracer Tests

The flow domain, including both the stream channel and hyporheic zone, consists of many different flow paths through which water and solutes can travel through. Some of these flow path velocities may be high-speed and others may be slower moving routes, and these paths are often temporally dynamic, changing based on flow conditions. The distribution of these paths under a given condition can be assessed through transit time distributions (TTDs) and residence time distributions (RTDs), which quantify the relative likelihood of water parcels following flow pathways characterized by different velocities. Moments, including the mean transit time (MTT) and skewness, and quartiles of the TTDs are metrics that can be used for comparative analysis among geographically and hydrologically differing flow domains (Headley and Kadlec, 2007; Hrachowitz et al., 2016). Quantifying and comparing the transit time distributions is useful for understanding the hydraulic performance and solute transport dynamics present in a flow domain, and provides metrics for pollution removal (Beckingham et al., 2019).

Tracer tests offer one method for quantifying the range of transit times that can exist within a system. This method has a long history of being utilized to characterize the TTDs and RTDs of natural and constructed wetlands, and stems from theory developed for chemical reactors (Headly and Kadlec, 2007). Idealized steady-state systems can be described as plug flow reactors or continuously stirred tank reactors. In the former, it can be envisioned that water and its constituents would flow through the wetland with no mixing, and any tracer added as a pulse would exit the system at the same time. In the latter, the water and its constituents are completely mixed and all parcels of water present in the system have an equal chance of leaving the system. For actual wetland and pond systems, flow is non-ideal, and the range of the transit time distributions can exist as a mix of the two ideal flows (Holland et al., 2004). In surface systems where advective transport is strong, tracer movement resembles movement of the water, but depending on the system, diffusion and mechanical dispersion will also act upon the tracer (Hrachowitz et al., 2016). Comparing the transit time distribution of systems under different conditions can give insight into the functioning of the systems and the spatiotemporal variability present in transport dynamics (Heidbüchel, et al., 2012).

Urbanization alters water transit and residence times, making it harder to quantify them in urban catchments. Water entering an urban catchment is convoluted due to a mix of old and new water infrastructure and impervious surfaces preventing infiltration and increasing runoff. In one study utilizing stable water isotopes, MTTs of an urban tributary were lower, though still ranging between 442 and 1764 days, when compared to a nearby rural tributary, while a site at the outflow of a sustainable urban drainage system had an MTT of eight days (Soulsby et al., 2014). Another study of transit times within SWMPs found that water entering was older than water exiting, and that surficial geology was a major influence on the MTTs of the SWMPs (Morales

and Oswald, 2020). Conservative tracer tests are often utilized in treatment wetlands where flow conditions do not vary by much. By utilizing conservative tracer tests to characterize TTDs of stormwater infrastructure in highly urbanized areas, we can further investigate another application of this method and add to the literature of quantifying transit times of reaches within urban catchments.

As urban areas are expected to expand and increase in population, there is a need to expand upon and diversify stormwater infrastructure and management practices. Beaver impoundments in rural landscapes have been shown to affect the flow and quality of water, but their ability to do this is less understood in urban landscapes. To address this knowledge gap, we organized a study with the following objectives: (1) measure the range of transit times that exist within the pond systems under different seasonal conditions, and (2) examine the possible relationships between pond geometric features and moments of the TTD. I hypothesize that the TTDs will have greater variance and transit times in dry conditions versus wet conditions. I further hypothesize that the MTTs of the TTDs will be positively related to flow path length from the inlet to outlet and pond area, while the MTTs will be inversely related to the prevailing gradient. By addressing these objectives, it will also allow us to compare transit time distributions between the pond types.

2 METHODS

2.1 Site Description

Our study design included a selection of sites across a regional spatial scale where overall physiography and climate were similar. The broader scope of this research project spans sites in the metropolitan areas of Atlanta, GA, Charlotte, NC, and Durham, NC, all of which lie within the Piedmont physiographic province of the southeastern United States. The focus of this thesis is on the Atlanta, GA sites. The Piedmont physiographic region is underlain predominantly by crystalline metamorphic rocks, especially variants of gneiss and schist, also with substantial areas of intrusive igneous granite. The bedrock is commonly fractured at the interface with the overlying regolith and at meters to tens of meters below, with fractures becoming uncommon at greater depths (Higgins et al., 2003). The regolith is made up of soil and saprolite, ranging in depth from zero at outcroppings sometimes found on ridgelines and interfluves, to more than 45 m in valley bottoms. The Piedmont is characterized by hills and valleys and a dense network of groundwater fed streams. Most groundwater is stored within the regolith under unconfined conditions and discharges to local stream channels (LeGrand, 1967; Daniel et al., 1989). Common land elevations among these three metropolitan areas range from 120 m to 330 m above sea level.

The climate for all sites is categorized as humid, subtropical. The average annual precipitation for Atlanta is 1270 mm, which is generally distributed uniformly throughout the year, although fall tends to be drier than the rest of the year. The average temperature in July is 27℃ and the average January temperature is 7℃ (National Weather Service, 2022). In general, cold-season precipitation across the Atlanta metropolitan area results from low-pressure frontal systems that deliver relatively low-intensity precipitation, but often with extended duration.

Warm-season precipitation commonly results from convective storms that deliver more localized and intense precipitation, but often of shorter duration.

Tracer studies were conducted at two beaver impounded channel sections, one channel section with beaver dam analog (BDA) installations, and two stormwater ponds within the Atlanta metropolitan area (Figure 1). Surface areas and distances reported for each site below are based on approximate estimates determined from Google Earth Pro. Water quality measurements and grab samples were taken every two weeks at the inflow and outflow of each site from March 2021 to March 2023. Samples were analyzed using ion chromatography (IC; Thermo Scientific Aquion Ion Chromatography System), and the averages and standard deviations of the measurements and ion concentrations were calculated (Appendix A). The following is a short description of each site, with a summary of site characteristics presented in Table 1.
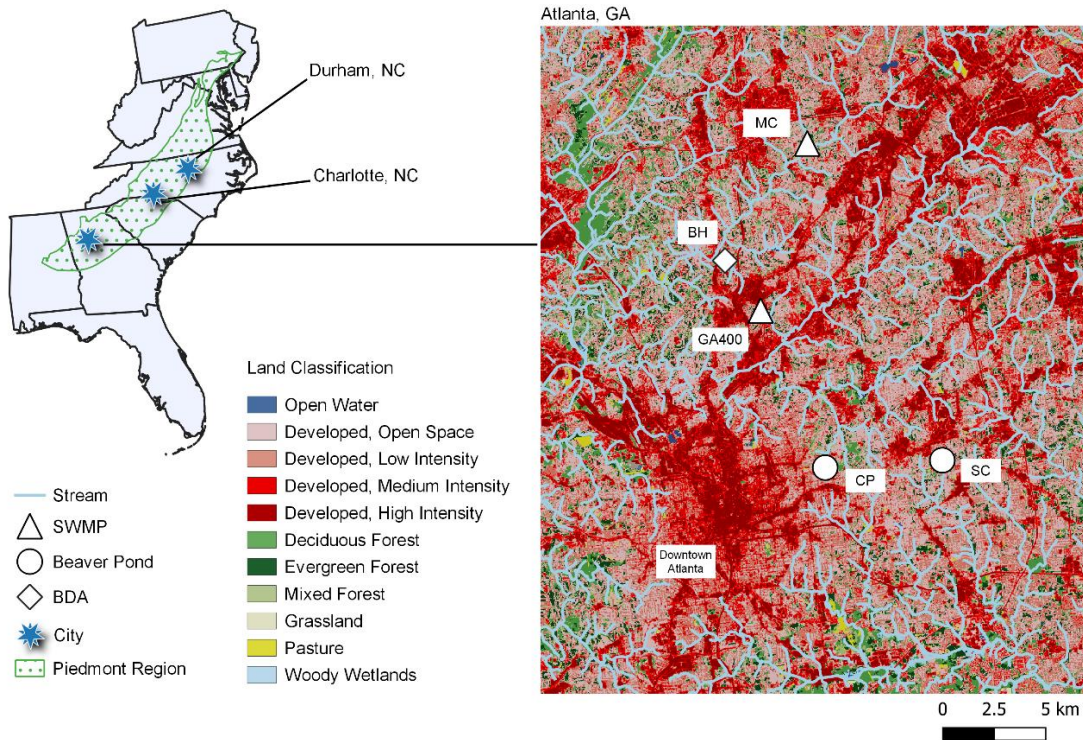
Figure 1: Map of site locations in the Piedmont physiographic region. SWMPs are indicated by a triangle, beaver dam sites are indicated by a circle, and the BDA site is indicated by a diamond. The land classifications in the background show the level of urbanization at each location.

2.1.1 Murphey Candler Park, Atlanta, GA

The SWMP at Murphey Candler Park is fed by North Fork Nancy Creek at its northern end and a smaller tributary at its eastern edge. The lake is the largest of all the sites with a surface area of approximately 78,000 m^2. Beaver have been reported at the site, though dam building activity is mostly confined within an adjacent wetland. Some beaver dams have been spotted in the North Fork Nancy Creek, but they are short lived due to high magnitude of stormflow. There were no perennial beaver-constructed structures in the portion of the creek and pond where our tests were conducted. The outflow is at the southwest point of the lake. It is a

rectangular concrete channel with a steep gradient that empties into a small stream. This stream flows for about 200 m before emptying into Nancy Creek and is surrounded by baseball fields. The direct path length from the main inflow to the outlet is 467 m.

2.1.2   Path 400 & Indian Creek Park, Atlanta, GA

This SWMP is located adjacent to the multi-use trail that is part of the PATH400 Metro Atlanta trail system. The GA 400 freeway and its earthen foundation forms its eastern edge. An elevated section of the MARTA railway lies just to the west. The main inflow may be a buried stream, since it flows year-round, and originates from the residential area to the west. It enters the pond through two culverts, though cracks in the culverts make it so the water flows from underneath rather than through, particularly during low flow conditions. During storm events, water is routed from the Georgia 400 freeway into the pond at its northern point. There appears to be another piped inflow at that point as well, but it may be disconnected because no water has been observed to flow from it. The pond is lens shaped and the surface area is approximately 9,900 m^2. The outflow is on the eastern edge of the pond, with a direct path length of 85 m from the main inflow. The water then flows underneath the Georgia 400 freeway where it emerges into a wooded park. While beaver are periodically active at this site, no colonies resided here while tracer tests were ongoing.

2.1.3   Shoal Creek, Decatur, GA

There are two beaver dams located on an unnamed tributary to Shoal Creek, near its headwaters at the eastern sub-continental divide that traverses DeKalb County, GA. Water flows out of a small, constructed pond called Postal Pond into a short reach of the creek that then flows into the beaver dam complex. The outflow from Postal Pond (i.e. the inflow to the creek and beaver-dam complex) emerges at a spill-over point on the earthen dam and varies temporally

with the water level in that pond. The beaver-dam complex has an approximate surface area of

3000 m^2 and the riparian area and adjacent hillslopes are forested. The estimated path length of

the pond is 116 m. A culvert runs underneath Katie Kerr Dr., the major road that borders the

beaver complex to the east, where the pond outflow converges back into the unnamed tributary

of Shoal Creek.

2.1.4   Candler Park, Atlanta, GA

The beaver pond complex at Candler Park lies within a golf course. The number of dams

present at this site fluctuates throughout the year, and over the course of the two-year monitoring

period has ranged from 0 to 3 dams due to apparent wash outs and subsequent rebuilding by the

beaver. The main inflow for the site is buried and flows directly into the first beaver pond of the

complex when constructed. The first dam seems to have the most beaver activity and is generally

repaired quickly after a dam failure. Two tributaries connect to the ponded channel just below

the first dam on the east and west sides. The western tributary is dry most of the year, flowing

mostly in the winter, while the eastern tributary is dry only in the summer. The irrigation system

at the golf course flows into the eastern tributary, which may enhance flow throughout the year.

Continuing downstream, the dams are more transient. The total surface area is estimated to be

about 4657 m^2 and the path length from inlet to outlet is about 157 m.

2.1.5   Blue Heron Nature Preserve, Atlanta, GA

Blue Heron Nature Preserve is 30 acres of woodlands, meadows, and wetlands. Beaver

have periodically built dams in Mill Creek, the stream that runs through the nature preserve, but

none have been reported in the park in recent years. In summer 2020, BDAs were installed along

an approximately 420 m stretch of Mill Creek. All but one have either fully or partially breached,

with extensive erosion occurring around the installations. Some ponding still occurs along the

stream reach, and the area is at least partially inundated with water in the late winter and into spring. The surface area of the reach is approximately 2100 m^2.

Table 1: Summary of site characteristics. The last four columns were components used to determine the amount of NaBr salt to be injected for the tracer tests. There are multiple spots where stormwater may be routed into the pond complex.

Site Name	Abbreviation	Site Type	Number of Perennial Inflows	Number of Intermittent/ Ephemeral Inflows	Area (m²)	Path Length (m)	Approximate Volume (m³)	Average Br⁻ Concentration at Outflow [a] (mg/L)
Murphey Candler Park	MC	SWMP	2	0	77902	467	194755	0.03 (0.01)
Path 400	GA400	SWMP	1	0	7433	85	14866	0.06 (0.02)
Shoal Creek	SC	Beaver	1	0	3014	116	3014	0.02 (0.01)
Candler Park	CP	Beaver	1	2	4657	157	4657	0.06 (0.02)
Blue Heron	BH	Beaver (BDA)	1	0	2100	420	3150	0.08 (0.04)

[a] The average Br⁻ concentration at the outflow was calculated from weekly samples taken over the two-year monitoring period, with the standard deviation listed in parentheses.

2.2   Data Collection

2.2.1   Stream Discharge and Precipitation

Water level within an installed stilling well was monitored at the inflows and outflows of each site (Onset HOBO U20L Water Level Logger) at 15-minute intervals. The water level loggers were installed in the spring of 2021, and continuously monitored sites over a two-year period. Discharge was measured using dilution gauging or an in-situ velocimeter, as described below.

For dilution gauging, a known mass of salt (NaCl) was instantaneously added to the stream and the change in conductivity was logged using a YSI probe downstream. The salt was added in a turbulent part of the stream and the length of the reach was approximately 10 times as long as the width of the stream to help ensure the salt fully mixed. During the tests, at least four samples were taken, including a pre-sample to establish the base concentration of chloride, a sample at peak conductivity, and samples in between. At some sites the breakthrough was rapid enough that one sample was taken across each of multiple tests. A conductivity-chloride concentration relationship was then established using data from all tests. Dilution gauging for each site was conducted over the same segment and as close to the water level logger as possible each time. Samples were analyzed by IC to quantify chloride concentrations. The exact time was noted when each sample was collected so the logged conductivity could be related to chloride concentration via linear regression. A breakthrough curve of the chloride concentration was then estimated using the fitted equation.

An in-situ doppler ultrasonic area/ velocity device (InSitu FloPro) was used to determine discharge at sites where the streambed and cross-sectional area made installation possible. It collected discharge measurements at 15-minute intervals for two to three weeks at a time to

cover a range of flows. It was installed at the sites at Murphey Candler Park, Candler Park, and Blue Heron.

USGS rain gauges were used to determine the amount of precipitation that occurred at each site in the week prior to tracer addition and the duration of tracer recovery. Each rain gauge was chosen based on distance from site and availability of 15-minute time series precipitation data. Rain gauge numbers and distance from site can be found in Table 2.

Table 2: The USGS rain gauge station used to collect precipitation data for each site and their approximate distance from each pond.

Site	USGS Rain Gage Number	Distance from Site (km)
MC	02336321	2
GA400	02336120	2
SC	02203950	5
CP	02203831	8
BH	02336360	0.5

2.2.2 *Quantifying Transit Times of Water in SWMPs and Beaver Ponds*

Tracer tests were performed to quantify the TTDs of water flowing through the different pond systems. Similar to many previous works in wetlands and large surface-water bodies [e.g., as reviewed by Headley and Kadlec (2007)], we selected Br^- (from dissolved NaBr salt) as an ion tracer because of its relatively low cost, high solubility, low ambient concentration in surface water, and low reactivity resulting in near-complete mass conservation during transport. Tests were performed in two sets. First, in the early fall (October 2021), when the watersheds were transitioning from their driest seasonal condition to wetter winter conditions. The second set of tests were conducted in early spring (April 2022) during the transition from wet, cold-season conditions to drier warm-season conditions (Aulenbach and Peters, 2017). It is understood that TTDs are variable in time due to temporal variability in the hydrological conditions of the flow

domain (Lewis and Nir, 1978). Performing the tests in these two periods allowed us to examine two relatively extreme conditions within that overall range of hydrological variability.

Ideally, the tracer would be introduced instantaneously at a point above the ponds. However, fairly large volumes of tracer solution are required for these tests, and instantly pouring them into these stagnant water bodies would create undesired, artificial hydraulic conditions. Instead, we approximated the plausible arrival time of dissolved Br^- at the pond outlets based on the linear distance from inlet to outlet and a coarse estimate of surface-water velocity. At each site, the tracer was injected into the systems as quickly as possible over a time increment that amounted to less than 1% of that approximated arrival time at the outlet. At many sites the tracer solution was pumped into the inlet at a rate of approximately 15-20 liters per minute. At larger sites, we slowly poured the solution into the inlet over several minutes. Tracer mass was weighed in the lab, and then tracer was mixed on site with stream water and the resulting solution was sampled. Tracer test samples were taken using an autosampler at the bottom of the complexes at all sites except for Murphey Candler, where samples were taken in person at less frequent intervals. Samples were returned to the lab for analysis of Br^- concentrations on an IC.

Samples selected for IC analysis were filtered using a 0.45 µm filter. A random sample was filtered again using a 0.22 µm filter, to ensure that resulting Br^- concentrations were not affected by filter pore size. Sample that was filtered through just the 0.45 µm filter had a Br^- concentration of 0.026 ppm and sample that was filtered through the 0.22 µm filter had a concentration of 0.022 ppm. These values were within the analytical error of 0.011 ppm associated with Br^- for that IC run. Individual stock solutions were used to make five anion standards, and continuing calibration verifications were made to assess machine drift over the

course of analysis. Additionally, two U.S. Geological Survey reference standards were used as external standards to confirm calibration.

Given a near-instantaneous injection of the conservative tracer, and good recovery of the tracer mass at the outlet, the resulting breakthrough curve (BTC) provides one discrete approximation of the so-called forward TTD (fTTD; hereafter just TTD) for water parcels flowing through the channel/pond complex (Nir and Lewis, 1978; Botter et al., 2010; Botter et al., 2011; Rinaldo, et al., 2011; van der Velde et al., 2012; Harman, 2015). This is shown mathematically in equation 1 below. The term on the left-hand side represents the probability density function for transit times (T), conditional upon a specific tracer-input time (t_i, i.e., the fTTD). The form of the TTD is conditional on the time of tracer introduction due to the contrasting meteorological and hydrological conditions that may follow a particular injection time, and which may modulate the ensemble of flow pathways and local velocities that water molecules and dissolved solutes may experience. The density function is equivalent to the derivative with respect to time of the cumulative probability distribution of transit times, conditional upon the same time of injection. Given the latter conditionality, the tracer introductions were performed at each site as close in time as possible, and under similar weather conditions to the greatest extent possible. This effort supports the ensuing assumption that any differences in TTDs observed across sites can be attributed to the contrasting flow pathways and water velocities (i.e., internal variability) rather than external sources of variability in transport (e.g., Kim et al., 2016).

$$\overrightarrow{p_Q}(T, t_i) = \frac{d}{dx}\overrightarrow{P_Q}(T, t_i) \sim \frac{C_Q(t)}{\int_{t_i}^{t_{end}} C_Q(t-t_i)dt} \qquad (1)$$

Establishing a good mass recovery is necessary to confirm reliability of results. Mass recovery was calculated by multiplying the solution to the integral in the denominator of the right-hand side of equation 1 by the integrating volume of flow through the system over the same time increment (Kilpatrick and Cobb, 1985). A summary of the tracer solution characteristics and tracer addition details for each site can be found in Table 3.

Logistical constraints prevent the tracer at each site from being injected exactly simultaneously, and even following injection, the sites are sufficiently far apart that they experienced different weather conditions during the period of monitoring the BTC. This reality is likely of most importance for comparisons of TTDs quantified at sites across metropolitan areas (Table 1). These inconsistencies may cause differences in the TTDs among sites that are attributable to time and weather variability (i.e., extraneous variables for our study objectives) rather than variability in the morphology, flow path complexity, and hydraulics of the different sites (i.e., the focal points of our study objectives). To minimize the possible confounding effects of these extraneous variables, we analyzed our BTCs as a function of time, and as a function of cumulative outflow from the channel/pond complexes (Niemi, 1977; Fiori and Russo, 2008; Kim et al., 2016). This is accomplished as shown below:

$$t_Q(t) = \frac{1}{\bar{Q}} \int_{\tau=0}^{\tau=t} Q(\tau) d\tau \qquad (2)$$

where t_Q is the "flow-transformed time", which is a function of actual calendar time t; $\bar{Q}$ is the average flow rate observed throughout the observation of the entire BTC; Q is the measured flow rate occurring at a particular transit time τ, where $\tau = f(t, t_0) = t - t_0$. The integral is computed from the first moment of tracer injection until the BTC is fully observed. This transformation mutes any differences in BTCs (and TTDs) among sites that may result from weather variability among the sites [a.k.a., external transport variability, (Kim et al., 2016)] and

ensuing differences in average flow rate of water within the channel/pond complexes. As such, remaining differences in BTCs and TTDs among sites can be more reliably related to differences in geomorphology, flow path complexity, and hydraulics.

Response variables for each tracer test were calculated for comparative analysis of the TTDs. These variables include the flow normalized first through third moments of each distribution (i.e., mean, variance, skewness) and selected intervals of probability (e.g., 25th versus 75th percentiles of transit time). The potential relationship between the response variables and the pond geometry, including flow path length from inlet to outlet, pond surface area, and the relief from inflow to outflow was explored through regression analysis. Pond geometry variables were approximated through Google Earth Pro. Due to the small sample size, response variables were lumped together rather than performing the regression analysis by seasons.

2.2.3   Error Calculations for Br⁻ Mass Flux

A plausible range of the mass recovery for each tracer test was calculated from the error present in the rating curves and the analytical error from the ion chromatograph. The error from the rating curve was determined by using the upper and lower 95% confidence coefficients of the rating curve variables. The absolute difference between the confidence boundary and the curve of best fit was taken to be the associated error for the calculated discharge at a given depth. The background Br⁻ for each site was determined by taking the average Br⁻ concentration of the weekly grab samples taken over an approximately two-year monitoring period. These concentrations follow a normal distribution, and the standard deviation was used for error propagations. The analytical error was determined to be three standard deviations of the continuing calibration verifications analyzed on each ion chromatograph run.

$$\Delta q = \sqrt{(\Delta x)^2 + (\Delta y)^2} \tag{3}$$

$$\frac{\Delta q}{q_{best}} = \sqrt{\left(\frac{\Delta y}{y_{best}}\right)^2 + \left(\frac{\Delta x}{x_{best}}\right)^2} \tag{4}$$

Error propagation was first calculated for the background corrected Br⁻ concentration using equation 3. The Br⁻ concentrations were interpolated at 15-minute intervals for the duration of the BTC, and then multiplied by the volumetric flow for that time increment to get the mass flux of Br⁻ for the 15-minute period. The error propagation for this calculation was determined by using equation 4. To determine the mass recovery, the total Br⁻ mass flux over the entire BTC was calculated. The associated error propagation could then be determined using equation 3 again.

Table 3: Summary of tracer tests conducted in the fall of 2021 and spring of 2022. The Br⁻ concentration listed here is calculated.

Site Name	Site Type	Date of Injection	Mass of NaBr (kg)	Mass of Br⁻ (kg)	Volume of Tracer Solution (L)	Br⁻ Concentration (ppm)	Injection Duration (min)	Tracer Solution Density (g/mL)	Number of Injection Points
MC	SWMP	10/13/21	10.0	7.8	360	21571	12	1.028	1
GA400	SWMP	10/13/21	2.9	2.3	360	6303	17	1.008	1
SC	Beaver	10/13/21	0.4	0.3	60	5215	3	1.007	1
MC	SWMP	4/1/22	20.0	15.5	480	32357	25	1.042	1
GA400	SWMP	4/8/22	2.9	2.3	360	6258	17	1.008	1
SC	Beaver	4/1/22	0.5	0.4	120	3236	10	1.004	1
CP	Beaver	4/1/22	1.3	1.0	240	4206	7	1.005	1
BH	Beaver (BDA)	4/8/22	0.5	0.4	120	3236	10	1.004	1

3   RESULTS

3.1   Precipitation and Streamflow During Tracer Test Periods

Meteorological conditions leading up to the fall 2021 tracer introduction were mostly dry. The 7-day antecedent rainfall for SC, GA400, and MC were 7 mm, 10 mm, and 19 mm, respectively. There was no rainfall the day preceding, or the day of, the tracer injection at any of the sites. The amount of precipitation over the duration of the fall tracer test varied by site. The BTC concluded most rapidly at SC, over a period of approximately 10 days. Over that time period, total precipitation across the three sites ranged from 0 mm to 2 mm. The BTC at GA400 concluded after approximately 32 days; over this time period an additional 27 mm and 36 mm of precipitation occurred at GA400 and MC, respectively. The BTC at MC concluded after 70 days, over which time there was an additional 70 mm of precipitation (Figure 2).

Tracer introduction for the spring 2022 tests occurred on two different days leading to varied meteorological conditions experienced across the sites. The 7-day antecedent rainfall for CP, SC, and MC, where tracer was introduced on April 1, 2022, were 15 mm, 16 mm, and 19 mm, respectively, all of it occurring on the day preceding tracer introduction. There was no rainfall on the day of tracer introduction at any site. The BTC concluded most rapidly at CP, over a period of approximately 4 days. Over this time period, total precipitation at the three sites ranged from 51 mm to 61 mm. The BTC at SC concluded after approximately 6 days; over this time period an additional 16 mm and 26 mm of precipitation occurred at SC and MC, respectively. The BTC at MC concluded after approximately 7 days, and an additional 2 mm of precipitation occurred (Figure 2).
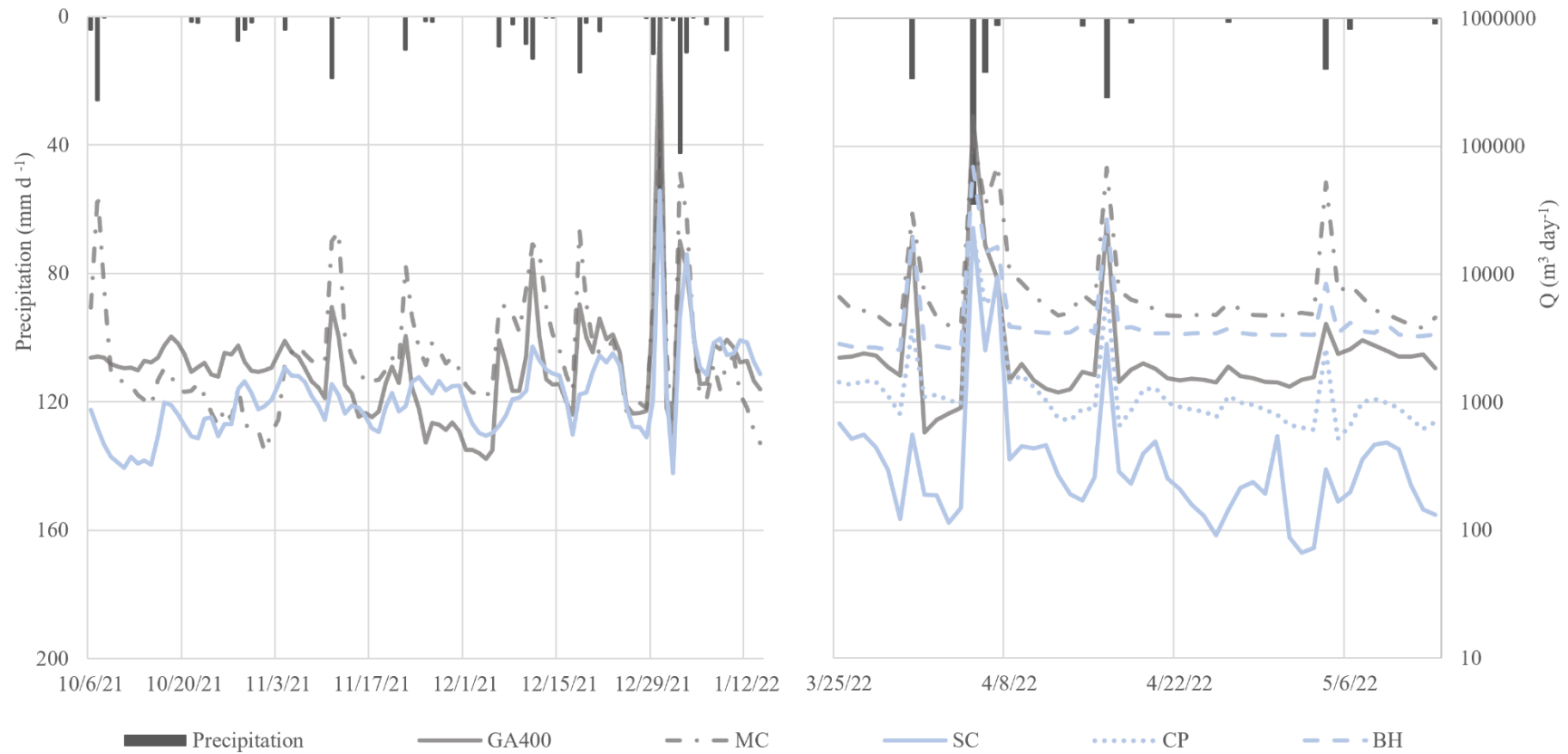
Figure 2: Time series of precipitation (mm d⁻¹) and streamflow (Q, m³ d⁻¹) occurring prior to Br⁻ tracer injection, and throughout the duration of the observable breakthrough curve, for those tests conducted during fall (left) and spring (right)—seasons with relatively dry and wet antecedent rainfall conditions, respectively. For graphical illustration, the time series from a single rain gauge is used here, although unique gauges that were most proximal to each site were utilized in other data analyses. Sites include GA400 and MC in-channel retention pond, the SC and CP beaver ponds, and BH BDA installation.

At the remaining two sites, BH and GA400, tracer was introduced a week later, on April 8, 2022. The later introduction at GA400 was due to an autosampler malfunction that required repair before initiating the test. The 7-day antecedent rainfall was 66 mm and 77 mm at BH and GA400, respectively. There was about 3 mm of rainfall at both sites the day preceding tracer introduction, while on the day of there was no rainfall. The BTC at BH concluded within 2 days. Over this time period no rainfall was recorded at either site. The BTC for GA400 concluded after approximately 16 days, over which time there was 27 mm of precipitation (Figure 2).

Flow duration curves displaying the mean-daily discharge rate (m^3/s) versus the exceedance probability at the pond outflows over the 2-year monitoring period were developed (Figure 3). Each site was monitored between the years 2021 and 2023. Mean daily discharge for this two-year monitoring period ranged from 4.0 x 10^{-4} m^3/s to 0.19 m^3/s, 0.02 m^3/s to 0.15 m^3/s, and 1.3 x 10^{-3} m^3/s to 0.38 m^3/s at the outflows of the SC, BH, and CP beaver pond sites, respectively. At the outflows of the stormwater retention pond sites, the mean daily discharge ranged from 4.6 x 10^{-3} m^3/s to 1.4 m^3/s at MC and 4.0 x 10^{-4} m^3/s to 0.49 m^3/s at GA400.

The flow duration curves give a deeper understanding of the specific flow conditions each tracer test encapsulates at each site. During the fall tracer tests, flows in the SC beaver ponded channel corresponded to exceedance probabilities ranging from 69% to 9%. Flows at the MC and GA400 retention ponds corresponded to exceedance probabilities ranging from 99.6% to 11% and 75% to 30%, respectively. In contrast, during the spring tracer tests, flow in the same beaver ponded channel corresponded to exceedance probabilities of 95% to 2%, while flows from the two retention pond sites had exceedance probabilities ranging from 46% to 2% and 74% to 24%. Additional spring tracer tests were conducted at the BDA restoration project at BH

and the CP beaver ponded channel. Exceedance probabilities ranged from 30% to 22% and 61% to 0.6%, respectively.
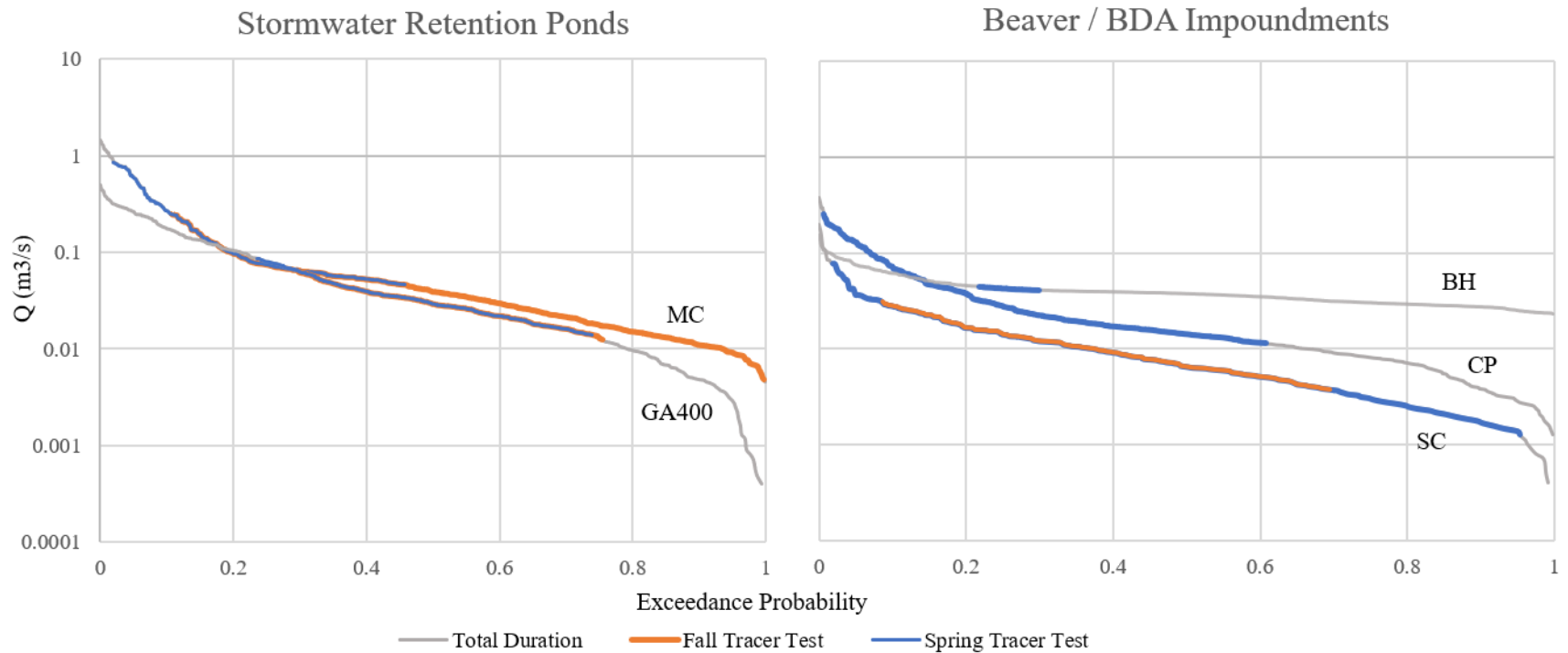
Figure 3: Probability of exceedance (i.e., flow-duration curves) for streamflow (m³ s⁻¹) at each of the four sites. The gray line represents these probabilities based on all measurements collected at 15-minute intervals between February 2021 and September 2022. The blue- and orange-highlighted portions of the plotted data indicate the range of flows observed during the Br⁻ tracer tests performed during the spring and fall seasons, respectively.
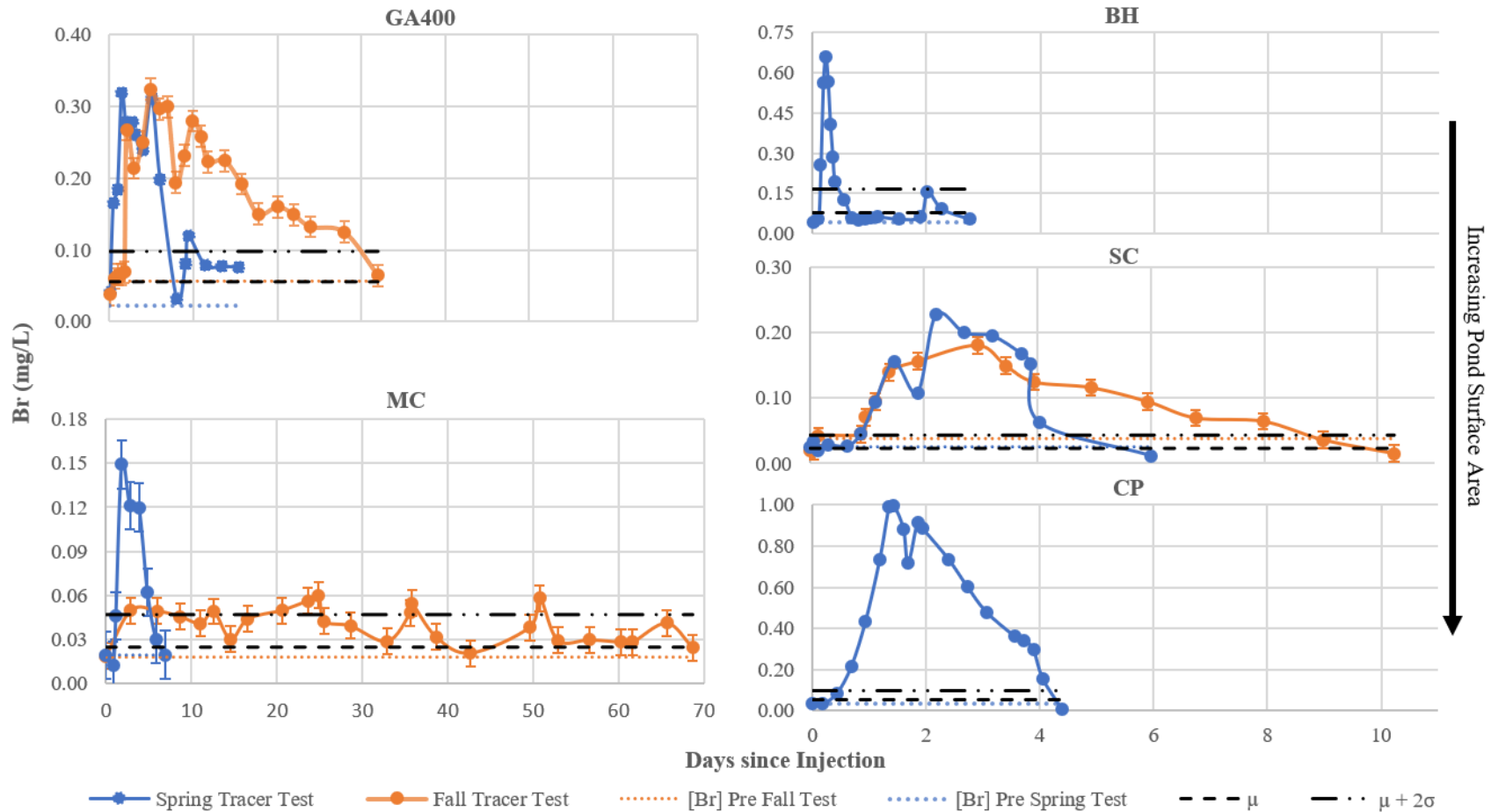
Figure 4: BTCs depicting the fall and spring tracer test results for SWMPs (left column) and beaver pond sites (right column), ordered by increasing pond area from top to bottom. The different methods for determining background Br⁻ concentrations are shown by the dashed lines. The different methods include using the initial Br⁻ concentration at the time of tracer introduction ([Br] Pre), the average Br⁻ concentration determined from weekly outflow sampling (µ), and the average Br⁻ concentration plus two standard deviations (µ+2σ)
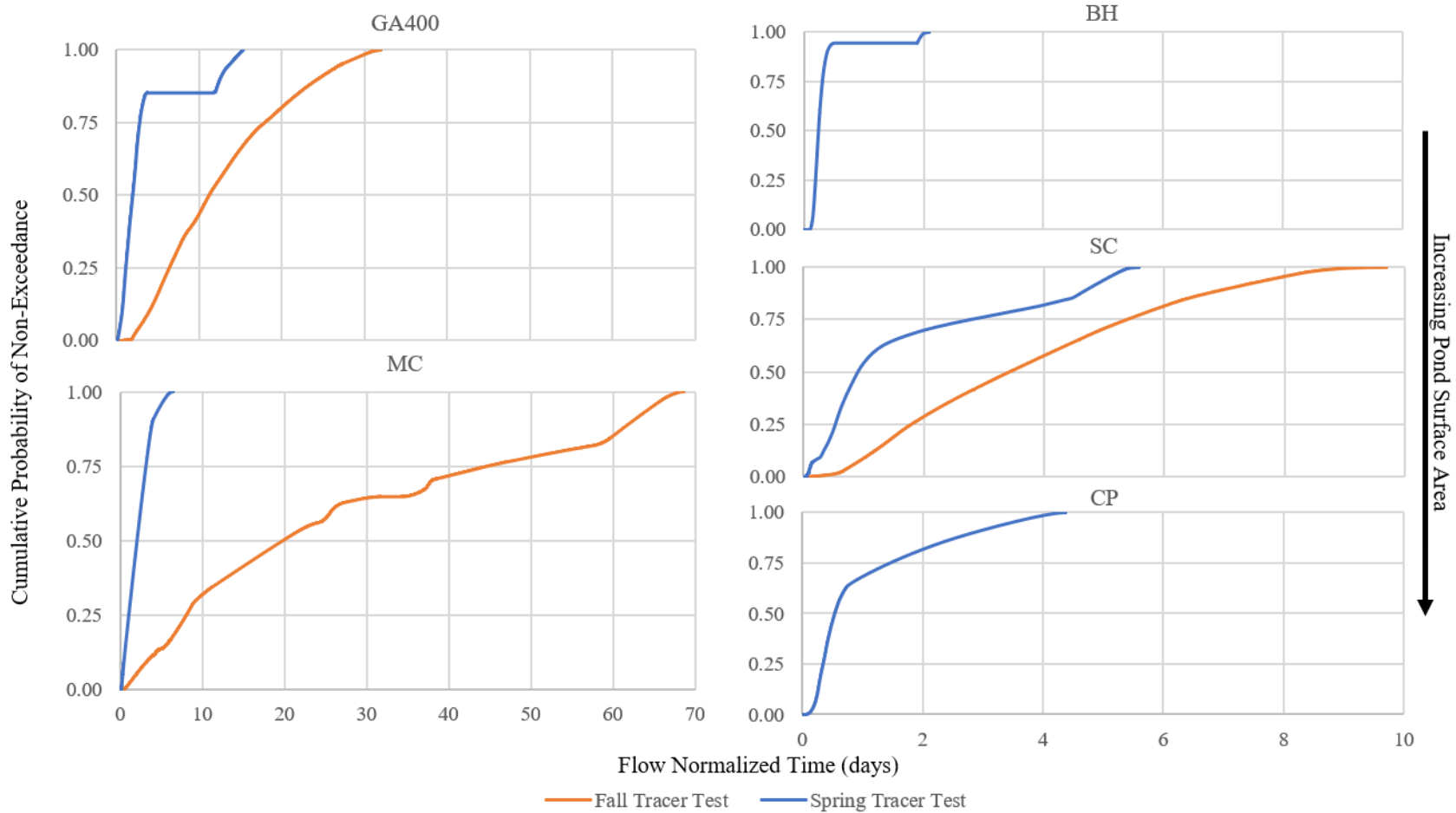
Figure 5: The TTDs for the introduced tracer expressed as cumulative probability of non-exceedance ordered vertically by increasing pond complex size. The results from the fall and spring tracer tests are depicted by the orange and blue curves, respectively.

3.2   Tracer Breakthrough Curves and Cumulative Forward Transit Time Distributions

The tracer BTCs show distinct seasonal characteristics between the sites. The fall BTCs for the GA400 stormwater retention pond and the SC beaver ponded channel have positive skews, while the MC stormwater retention pond BTC appears multi-modal with no distinct peak (Figure 4). The time to peak concentration following tracer introduction is delayed when compared to the spring BTCs across the three sites where fall tracer tests were performed, and at MC and SC, the curves are flatter when compared to their spring counterparts (Figure 4). The flow normalized transit time distribution curves further show the predominantly steady release of tracer over the duration of fall tests, and a more rapid release in the spring with some tailing behavior (Figure 5). The maximum signal to noise ratios for the fall BTCs ranged from 1.40 at MC to 7.83 at SC (Table 4).

The BTCs for the spring tracer tests are more uniform in shape. The BDA installation at BH and the stormwater retention pond at GA400 are bi-modal, and all the sites appear to have little to no skewness. For the three sites at which seasonal comparisons can be made, MC, GA400, and SC, Br^- concentrations returned to background levels much more rapidly in the spring tests than in the fall (Figure 4). The maximum signal to noise ratios for the spring BTCs ranged from 4.33 at GA400 to 16.50 at CP (Table 4).

Under the dry climatic conditions experienced during the fall tracer tests, the total range of Br^- transit times within the ponds was approximately 10 to 69 days. The total range of transit times of the Br^- tracer was 9.8 days at the SC beaver pond. The transit times of the Br^- tracer was 68.6 days and 32.0 days at the MC and GA400 stormwater retention ponds, respectively (Figure 4).

Under the wetter climatic conditions experienced during the spring tracer tests, the total range of transit times was markedly lesser, spanning only approximately 2 to 15 days across sites. The transit times of the Br^- tracer was 1.5 days, 5.6 days, and 4.3 days at the BH, SC, and CP beaver ponds, respectively. The transit times of the Br^- tracer was 6.4 days and 15.4 days for the MC and GA400 stormwater retention ponds, respectively (Figure 4).

Tracer mass recoveries were calculated for each tracer test in the fall and spring. Fall tracer mass recoveries for MC, SC, and GA400 were 31%, 140%, and 386%, respectively. Spring tracer mass recoveries for MC, GA400, BH, SC, and CP were 77%, 98%, 106%, 223%, and 305%, respectively. Based on the error in the rating curves and error in the instrument, a plausible range of mass recovery was calculated for each tracer test (Table 4). The calculated mass recovery for GA400 in the spring is within this plausible range.

Table 4: Details of the tracer mass added and recovered for all tracer tests performed. The plausible range of mass recovery is based on error-propagation approximations considering the error from the rating curves and instrument analysis.

	Stormwater Pond Sites				Beaver Pond Sites			
	GA400		MC		SC		CP	BH
	Fall	Spring	Fall	Spring	Fall	Spring	Spring	Spring
Br^- Added (kg)	2.30	2.30	7.80	15.5	0.31	0.39	1.00	0.40
Lower Recovery Range (kg)	1.92	2.09	7.69	14.5	0.31	0.33	0.71	0.37
Br^- Recovered (kg)	8.75	2.20	2.39	11.9	0.43	0.55	3.05	0.41
Upper Recovery Range (kg)	2.68	2.41	7.91	16.6	0.32	0.44	1.29	0.40
Mass Recovery (%)	386	98	31	77	140	223	305	106
Signal to Noise Ratio	4.33	4.33	1.40	6.00	7.83	10.0	16.5	8.25

3.3 Moments and Quartiles of the Forward Transit Time Distributions

The moments of the TTDs offer one method of comparison between sites and seasonal conditions. Under the drier fall conditions, the MTTs, for the stormwater retention ponds at MC

and GA400 were 36.6 days and 12.5 days, respectively, while the MTT for SC was 4.5 days. While this set of tracer tests were carried out within the same day, and therefore experienced similar meteorological conditions initially, time and weather variability as the tests proceeded create time-varying flow conditions that variably affected the BTCs across sites. The flow-normalization procedure described in the methods helps remove this external source of transport variability, so that remaining contrasts in TTDs can be more reliably attributed to in-channel/in-pond flow and transport processes. The MTTs for the same sites when normalized for outflow are 26.6 days, 12.7 days, and 3.7 days, respectively. The relative magnitudes of the flow-normalized MTT at MC is qualitatively different than the MTT noted above. The flow-normalized MTT at MC is almost 1.5 times smaller than the MTT, suggesting that, despite its greater size, the flow through MC may occur preferentially along a constrained set of pathways.

Under the wetter, spring conditions, MTTs were reduced to 4.2 days at MC and 4.5 days at GA400. The SC site had less of a reduction in its MTT at 4.1 days. The flow normalized values were 2.2 days, 3.4 days, and 1.8 days at MC, GA400, and SC, respectively. Additional tracer tests were performed at the BDA installations at BH and the beaver ponded channel at CP in the spring. These sites had MTTs of 0.4 days and 2.8 days, while the flow normalized MTTs were 0.4 days and 3.7 days, respectively.

A difference between the MTT and median value is indicative of skewness in the TTD. Generally, a skewness value between -1 and 1 would indicate little no skewness in the distribution. The median values for the tracer tests performed in the fall were 29.6 days, 10.7 days, and 4.4 days at MC, GA400, and SC, respectively. In the same order, these sites had a skewness of 1606, 304, and 1.5. In flow normalized time, the median values for MC, GA400,

and SC were 20.3 days, 11.2 days, and 3.4 days, with corresponding skewness values of 6217, 262, and 5 for each site.

The median values for the spring tracer injections conducted on April 1, 2022 were 4.2 days for both MC and SC and 2.8 days for CP. In the same order, the sites had a skewness of -0.35, -0.43, and -0.30. For the tracer tests that began on April 8, 2022, the median values were 3.9 days at GA400 and 0.2 days at BH, with associated skewness values of 48.0 and 0.22. In flow normalized time, the median values for MC, SC, and CP were 2.0 days, 0.8 days, and 0.9 days, with corresponding skewness values of 1.4, 4.3, and 35.4. For GA400 and BH, the flow normalized median values were 2.0 and 0.2 with skewness values of 140 and 0.22, respectively. Other metrics calculated to compare the shapes of the TTDs can be found in Table 5.

Table 5: Descriptive statistics for the fall and spring TTDs. Descriptive statistics include the first through third quartiles, the first three moments, and the standard deviation in days (top) and flow normalized days (bottom).

	1st quartile	Median	3rd Quartile	Total Duration	Mean	Standard Deviation	Variance	Skewness
				Fall				
MC	25.2	30.0	55.8	68.7	36.6	6.05	353	1610
GA400	5.65	10.7	17.9	32.0	12.5	3.54	60.2	304
SC	3.34	4.41	5.64	9.81	4.46	2.11	3.23	1.54
				Spring				
MC	4.07	4.15	4.28	6.41	4.19	2.05	0.49	-0.35
GA400	1.83	3.86	5.91	15.4	4.54	2.13	11.5	48.0
SC	4.17	4.19	4.23	5.57	4.13	2.03	0.22	-0.43
CP	1.74	2.77	4.11	4.27	2.84	1.68	1.40	-0.30
BH	0.20	0.24	0.31	2.09	0.35	0.59	0.15	0.22

Flow Normalized Days

	1st quartile	Median	3rd Quartile	Total Duration	Mean	Standard Deviation	Variance	Skewness
				Fall				
MC	8.87	20.3	42.2	68.7	26.6	5.15	439	6220
GA400	6.36	11.2	17.8	32.0	12.7	3.56	57.0	262
SC	1.78	3.40	5.37	9.70	3.74	1.93	5.00	5.19
				Spring				
MC	1.03	2.02	3.09	6.44	2.24	1.50	1.87	1.42
GA400	1.12	1.95	2.80	15.4	3.36	1.83	17.3	139
SC	0.50	0.80	2.50	5.58	1.83	1.35	2.81	4.32
CP	0.34	0.53	1.44	4.38	1.08	1.04	1.22	1.90
BH	0.20	0.24	0.31	2.09	0.35	0.59	0.16	0.23

3.4 Relationship between Pond Geometry and Moments of the Transit Time Distributions

Simple linear regression analysis was performed to explore the relationship between key pond geometries and the moments of the transit time distributions. Independent variables included the relief, path length from inlet to outlet, the relief divided the path length as a proxy for slope, the surface area of pond, and the relief divided by the path length and surface area of

the pond. The dependent variables included MTTs, variance, the median transit time, and

interquartile ranges. R-squared values for the regression models indicate that most of the

variance for the transit time distribution moments could not be explained by the selected pond

geometries (Table 5). Skew as a function of path length yielded the greatest R-squared value at

0.25 (Figure 6).

Table 6: The R squared values for all the linear regression analyses performed.

	MTT	Variance	Skew	Q1	Median	Q3	Interquartile Range
Relief (m)	0.13	0.19	0.19	0.09	0.19	0.15	0.16
Path Length (m)	0.08	0.21	0.25	0.04	0.08	0.10	0.18
Relief / Path Length	0.07	0.16	0.18	0.03	0.16	0.10	0.13
Relief / (Path Length) (SA)	0.12	0.13	0.12	0.10	0.13	0.13	0.13
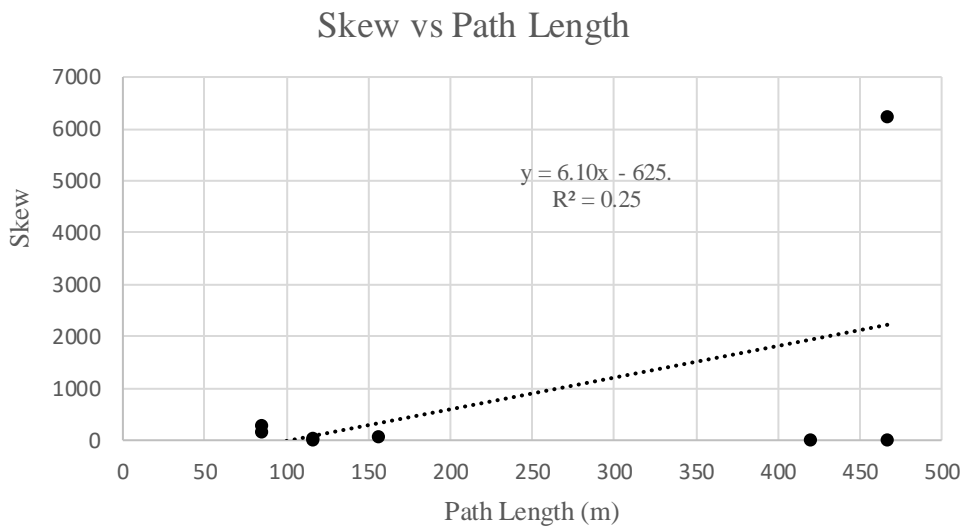
Figure 6: Selected regression analysis showing the flow normalized skew as a function of path length from inlet to outlet. Correlation was weak between moments of the TTDs and pond geometries.

4   DISCUSSION

4.1   Mass Recovery in Conservative Tracer Tests

The tracer mass recovery is a calculation that checks the reliability of the tracer test data. Acceptable ranges of tracer mass recovery given experimental error can be determined (Headley and Kadlec, 2007). For this study, this range was determined through error propagation calculations using the error associated with the rating curves, background Br^- concentration, and the IC instrument. From these calculations, only the spring GA400 test had a tracer recovery within this range. The other tests had tracer mass recoveries that ranged from 31% to 386%.

Other studies that have utilized Br^- as a tracer (from KBr, LiBr, and NaBr) were often examining either constructed or natural wetlands with pond areas similar to the ones included in this study, with the exception of the MC retention pond site which is much larger. Mass recoveries from these past studies include: a relative low of 40% in a 15,000 m^2 natural wetland within a rainforest preserve (Kaplan et al., 2015); an average of 86% in eight mine water treatment systems that range in size from 375 m^2 to 7388 m^2 (Kusin et al., 2014); 94% in a 2984 m^2 constructed wetland receiving water from an agricultural field (Pugliese et al., 2020); recoveries of 41% and 97% in two separate tests for a 258 m^2 constructed wetland in a agriculture area (Schuetz et al., 2012); and recoveries between 72% and 111% in constructed wetlands ranging from 100 m^2 to 215 m^2 in an agriculture dominated catchment (Gaullier et al., 2020). In a series of tracer tests conducted in wetlands constructed to improve river water quality, two methods of calculating mass recoveries were explored, using mean daily discharge and dynamic discharge (Kadlec, 1994). Calculations using mean daily discharge yielded values ranging from 85% to 121%, while calculations using dynamic discharge ranged from 56% to 112%. Mass recoveries on the lower end in these studies were explained as inadequate sampling

durations. Mass recoveries of over 100% were attributed to error in discharge determination, and it was concluded that mass recoveries were sufficient for further analysis to be carried out.

The lower mass recoveries reported for the MC fall and spring tests (31% and 77%) could be due to long term solute storage or the Br^- behaving non-conservatively due to plant uptake. The latter was shown to be the probable cause of low Br^- recovery in a wetland study (Whitmer et al., 2000), but does not seem to be a likely cause for our study since there was a higher mass recovery in the spring test, when there was denser vegetation. It is possible that there is more transient storage available within this pond compared to our other sites, and the last of the Br^- tracer was released at such low quantities that it was confounded with background levels of Br^- (e.g., as discussed by Drummond et al., 2012). The low mass recovery from the fall MC test may also be a consequence of not enough tracer mass being added. The mass of NaBr added was increased from 10 kg in the fall to 20 kg in the spring.

Possible causes for the higher mass recoveries, which was the more common issue for this study, are error stemming from the water level loggers and not correctly characterizing the background Br^- concentrations. It was found that the HOBO U20-L water level loggers used to measure the outflows at each site had a temperature induced error in the pressure readings (Moore et al., 2016; and unpublished data from our own field tests). This caused a diurnal signal where discharge was artificially lower during the warmer day time, and higher during the cooler night. A bias in the sampling time could therefore cause mass flux calculations to be biased low or high. While further efforts to remove this temperature-induced bias are underway, a method is still being developed and corrections to the depth time series have not been applied in this thesis. The background Br^- concentration for each site was determined by taking the average concentration of the weekly grab samples at the outflow. Samples tended to be taken during

baseflow conditions, and exclusively during daylight hours. If more stormflow samples are collected, then a baseflow separation method could be used to determine background Br$^-$ concentrations under baseflow and event flow conditions.

We proceeded with analysis of TTDs under the assumption that error associated with imperfect mass recovery is not time dependent, and instead equally distributed through the duration of the tracer test. For the cases where mass recovery was less than 100%, this assumption implies that if 100% mass recovery were achieved, the breakthrough curves in Figure 4 would look qualitatively similar, just uniformly scaled upward on the vertical axis. For the cases when mass recovery was greater than 100%, the assumption implies that the breakthrough curves would look identical to those in Figure 4, just uniformly scaled downward. Under this assumption, the appearance of the TTDs and cumulative TTDs—both flow normalized and un-normalized—is putatively identical to the forms that would have been observed if perfect mass recovery were achieved.

4.2   Seasonal Differences in TTDs within the Stormwater Retention Ponds and Beaver Ponded Channel

The tracer test results discussed here are part of a larger set of tests conducted across two other cities in the Piedmont physiographic region. While the sample size is small, this discussion aims to highlight observed patterns in the tracer tests conducted at the Atlanta sites. I hypothesized there would be observable differences in the form of the TTDs between seasonally dry and seasonally wet hydroclimatic conditions – those conditions being assumed to exist during the fall and spring seasons, respectively. Greater flow rates during wet conditions were hypothesized to cause a smaller range in transit times (i.e., a TTD with lesser variance), while

under dry conditions there would be a greater range in transit times (i.e., a TTD with greater variance).

Tracer tests were conducted in the fall of 2021 and spring of 2022 to capture seasonal differences in storage of the pond systems. The flow duration curves, developed from mean daily discharge values at the outflows of the pond systems, however, shows that the flow was not systematically lower in the fall. Assuming there is a positive relationship between outflow and the volume of water stored in each pond, then we can also infer that water storage was not systematically lower in the fall. Greater water storage would correspond to a broader wetted perimeter of the pond/channel and likely a broader array of flow pathways for water to take to the outlet. Yet, among the sites where tracer tests were conducted both in the fall and spring, MC was the only site where hydrologic conditions were distinct between the seasons. For the GA400 flow duration curve, there is considerable overlap of mean daily discharge rates during the tracer tests, and the hydrograph shows that peak daily discharge values and baseflow values were similar across seasons.

The spring tracer test at SC encompassed a greater range of mean daily discharges at bother lower and higher exceedance probabilities than in the fall. The hydrograph for SC shows that baseflow was lower in the spring than in the fall tests, when climatic conditions are typically drier. Beaver dams in forested and montane catchments have been shown to generally increase low flows and serve as a net source of water under drier conditions (Nyssen et al., 2011; Wegener et al., 2017). However, the earthen, human-constructed dam that creates Postal Pond and controls the inflow into the beaver impounded reach at SC had been widened and reinforced about a month before spring tracer injection and may be the reason for the lower daily outflow discharge rates seen in the spring hydrograph. These comparisons show that the difference in the

range of discharges observed at the outflow of the pond systems is more attributable to the short-term (i.e., hourly to daily) weather dynamics, rather than seasonal changes in storage. Any filling and emptying of transient storage within these channels/ponds appear to occur over those relatively short time scales.

The shapes of the flow duration curves also give insight into the behavior of the pond systems over the 2-year monitoring period. The BH curve is flat, with the curve only becoming steeper for the highest mean daily discharge values. A low prevailing slope in the plotted data indicates relatively large changes in cumulative probability of occurrence (horizontal axis) over relatively small changes in discharge (vertical axis), that is, the outflow/ streamflow is consistently low most of the time, and those low flows span a relatively small range of values. In contrast CP and SC have steeper slopes at the lower and upper end of the flow duration curves, showing more variability in the lower exceedance probability of mean daily discharge.

MC behaved similarly to CP and SC for the mean daily discharges with the highest exceedance probabilities but has more variability in the lower exceedance probability range. This could mean less storage capacity for higher discharge values. The GA400 curve has the steepest slope of all the sites at the lower exceedance probabilities values and is not as flat throughout in comparison. This is indicative of more variability in the mean daily discharge at the outflow of the pond.

Despite many sites not showing a difference in flow between seasons, the total durations of the breakthrough curves were all longer in the fall than in the spring. The greatest difference occurred at MC, where Br^- concentrations returned to the average background level after 69 plus days in the fall test and 6.4 days in the spring. GA400 saw a reduction from 32 days to 15 days, and SC was reduced from 10 days to 6 days. This is consistent with other studies that examined

the performance of constructed wetlands under high and low flowrates (Gaullier et al., 2019; Gaullier et al., 2020). As noted before, these changes seem to be mostly tied to short term weather dynamics. At MC, while there was more rainfall over the course of the fall tracer test, there was very little precipitation within the first two weeks. In contrast, precipitation was recorded within 4 days of spring tracer addition. GA400 experienced similar amounts of rainfall over the duration of both tests, but similar to MC, the precipitation in the spring occurred much sooner to tracer addition. SC had no precipitation during the fall test, and 77 mm during the spring. Our results support theoretical arguments (e.g., Lewis and Nir, 1978) and other tracer studies in surface-water bodies (e.g., Harman et al., 2016) demonstrating the pronounced temporal variance of solute and water TTDs.

I also hypothesized that the range in TTDs would be greater in beaver ponds than human built stormwater ponds, informed by field observations that the beaver ponds have more complex fluvial systems, with higher contact between water and sediments and a greater extent of hyporheic exchange. When comparing across site types, the stormwater retention pond sites had longer transit times than the beaver pond sites in both the fall and spring tracer tests. However, at MC and GA400 the flow normalized MTTs experienced in the fall versus the spring decreased by 92% and 73%, respectively, while at SC there was a 51% decrease. The faster spring transit times seen in the stormwater retention pond sites are in line with previous studies that show there is a precipitation threshold at which BMPs become less effective at managing stormwater (Sun et al., 2014; Miller et al., 2021). The ability for beaver dam complexes to attenuate flow is, in part, dependent on the topographical characteristics and antecedent storage conditions of the ponds (Neumayer et al., 2020; Westbrook et al., 2020; Graham et al., 2022). Landscapes that allow for the lateral expansion of ponds to store event volume and ponds that are already partially full on

the onset of storms has been found to allow for more effective flow attenuation. In Puttock et al.
(2020), it was even seen that at more mature beaver dam complexes, there was greater flood flow
attenuation under wetter conditions than dry. While the reduction in the MTT was not as
dramatic at the SC beaver site when compared to the stormwater retention pond sites, there still
appeared to be less flow attenuation at the SC site in the wetter season.

The shapes of the flow normalized TTDs show variation in the flow path configurations
between fall and spring tracer tests (Figure 7). In the fall, when all tests were performed on the
same day, there are similar transport dynamics between the two site types. The slope generally
changes gradually over the duration of the tracer test, with no inflection points. The exception to
this is at approximately 80% cumulative probability of non-exceedance at MC where the curve
does steepen. The gradually changing slope indicates transport dominated by mechanical
dispersion and diffusion (Gaullier et al., 2019). Under the low flow conditions that characterized
the first week after tracer addition, tracer was transported from the main flow channel to a larger
volume of the pond systems, increasing transit times. In Kaplan et al. (2015), a similar tracer
study was conducted in a constructed wetland where a high intensity storm occurred later during
the tracer recovery. It was suggested that the rainfall may have led to altered flow path
configurations over small spatial scales. At MC the steepening of the curve corresponds to a
precipitation event where the increase in inflow may have mobilized tracer that had been
immobilized in dead zones of the pond.

In comparison, the shapes of the spring flow normalized TTDs show stronger advective
transport of the tracer (Figure 7). Two distinct shapes in spring time TTDs arise, with one shape
corresponding to the tests that began on 4/1/22 and the other to the tests that began on 4/8/22.
For the earlier set of tracer tests, MC, SC, and CP, the initially steep slopes are indicative of a

relatively greater influence of advection, rather than diffusion, in transporting tracer mass toward the outlet. An inflection point at approximately 90% cumulative probability of non-exceedance at MC and 60% at both SC and CP indicates the influence of diffusion and mechanical dispersion on tracer transport. The tests where tracer addition occurred on 4/8/22 are also characterized by initially strong advective transport, but with an observed flattening of the curve at approximately 80% and 90% cumulative probability of non-exceedance at GA400 and BH, respectively. This feature of the cumulative TTDs results from outflow samples where Br$^-$ concentrations were at the established background level. The slope then becomes steep again, indicating the existence of a second, slower velocity flow path that tracer may have travelled along. The decrease in the flow normalized variance values in the spring tracer tests further supports that tracer transport was flushed through the pond systems with little hydrodynamic dispersion (Kadlec, 1994).
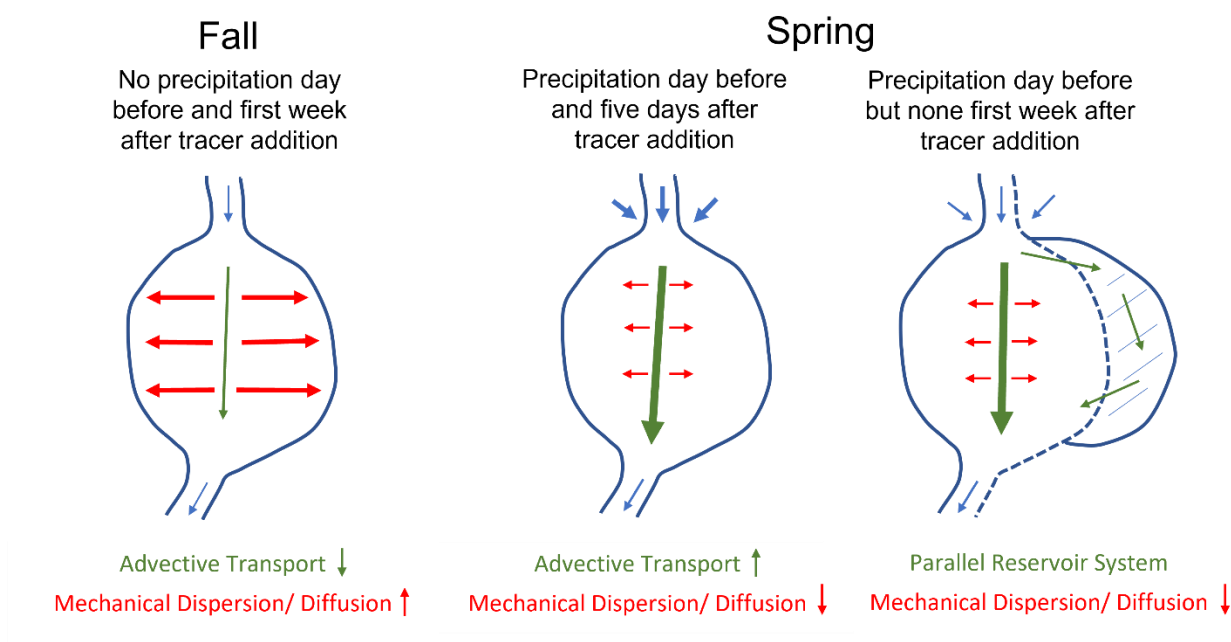

Figure 7: Conceptual diagram of tracer transport through the pond systems for the different precipitation conditions experienced in the fall and spring tests.

4.3   Relationship between Quartiles and Moments of the TTDs and Pond Geometry

I hypothesized that the variability in the seasonal TTDs would be a function of the geometry of the pond, including the flow path length from the inflow to the outflow and the configuration of the surrounding landscape, i.e., the pond's ability to expand and contract. While MC and GA400, the two stormwater retention pond sites, were the largest sites by surface area and approximate volume, the path lengths varied so that MC had the longest path length and GA400 had the shortest out of all of the sites. It was then envisioned that due to the variety in shapes and inflow/ outflow configurations the sites exhibit, factors beside pond volume may effect the shape and moments of the TTDs. Regression analysis performed between the moments and quartiles of the TTDs and different pond geometry metrics showed no clear relationship, though, with all the R-squared values equaling less than 0.3.

The pond size alone does not seem to be the only driver on the range of transit times in the ponds, as the MTT, first quartile, and total duration at GA400 were all longer than MC's in the spring. This differs from the fall results, where all moments and quartiles were longer at MC when compared to GA400. Similarly, it was estimated that CP had the largest pond area out of the beaver site types, but SC had a greater range in transit times and MTT for the spring set of tests despite the two having similar path lengths. The surface area estimates were made from Google Earth Pro images, and so a potential change in pond size between seasons, or in the case of the beaver pond systems, a change due to dam building or removal were not factored into the regression analysis. The length to width ratio, topography, and inflow/outflow configurations are design elements often cited when considering the hydraulic conditions of treatment pond systems (Persson and Wittgren, 2003). In more complex systems, flow velocities, variations in pond depth, sediment deposition, and vegetation cover have also been found to further influence

hydraulic performance (Holland et al., 2004; Laurent et al., 2015; Nuel et al., 2017; Gaullier et al., 2020). While some of these design elements were factored into the chosen metrics for the regression analysis, many were not. With a larger sample size from tracer tests conducted in Durham and Charlotte, NC, separate regression analysis for the seasonal tracer tests can be performed, which should help with any confoundment from the different flow velocities. Depth, potential changes in pond volume and size, and vegetation especially in the beaver ponds, could also be considered for a more robust analysis.

5   CONCLUSION

A total of eight Br⁻ tracer studies were conducted at two stormwater retention pond sites and three beaver/BDA ponded streams in the fall of 2021 and spring of 2022 in the Atlanta metropolitan area. It was expected that conducting the tracer studies under different climatic conditions, drier in the fall and wetter in the spring, would capture different seasonal flow conditions and that low flow conditions would have a greater variance in transit times. However, multiple sites did not show a seasonal difference in flow, obfuscating this analysis. Instead, I found that recent antecedent precipitation conditions strongly impacted the transit times. In the fall tests, when there had been no rain in the day preceding tracer addition and none within the first week after the addition, tracer was released from pond systems gradually, with strong mechanical dispersion and diffusion, regardless of pond type. In the spring, two distinct patterns could be seen in the tracer transport. Strong advective transport of tracer could be seen in all spring transit time distributions, but tracer tests performed a week later showed different transport dynamics. This suggests that all systems are sensitive to short term weather dynamics causing variability in the flow path configurations although for both the fall and spring tracer tests, tracer transit times were longer in the stormwater retention pond sites in comparison to the beaver ponded sites. Both stormwater retention ponds and urban beaver ponds may not be as adept at storing water during higher intensity precipitation events.

Regression analysis was performed to evaluate relationships between certain pond geometric features and moments of the TTDs. The human-built SWMPS, which are larger than the beaver ponds included in this study, had longer transit times, but the tests were inconclusive. Other, more nuanced characteristics of the ponds, such as depth or the ability for the pond to expand or contract, may need to be explored to resolve the predictive relationship with TTDs.

Tracer tests were also performed in stormwater retention pond and beaver pond sites in Durham and Charlotte, North Carolina and with a larger sample size, regression analysis conducted with the same metrics used in this study, as well as the more nuanced metrics, may be more conclusive.

Conducting tracer tests offers one way of quantifying the transit times and hydraulic conditions that exist within a pond system. Evaluating these temporally variable features can give insight into the pond's ability to store water, transport contaminants, and improve water quality. As alternative and complementary methods to more traditional stormwater management infrastructure become more popular, we sought to compare the TTDs of urban beaver ponds to SWMPs to assess the former's potential as a possible stormwater management method. The beaver ponds did not show the same ability to increase transit times as the SWMPs, regardless of flow conditions, though the beaver pond experienced less temporal variation in its transit times and the beaver ponds do not appear to be systematically different from the SWMPs. While rural beaver ponds have been shown to attenuate flow and increase water residence times, the urban environment does seem to limit this ability. This is an important consideration when evaluating the integration of beaver ponds into stormwater management plans.

REFERENCES

Aulenbach, B. T., Peters, N.E. (2018). Quantifying climate-related interactions in shallow

    and deep storage and evapotranspiration in a forested, seasonally water-limited

    watershed in the southeastern United States. *Water Resources Research*, *54*(4), 3037-

    3061, doi:10.1002/2017wr020964.

Beckingham, B., Callahan, T., Vulava, V. (2019). Stormwater Ponds in the Southeastern U.S.

    Coastal Plain: Hydrogeology, Contaminant Fate, and the Need for a Social-Ecological

    Framework. *Frontiers in Environmental Science*, *7*, 117.

    https://doi.org/10.3389/fenvs.2019.00117

Bailey, D. R., Dittbrenner, B. J., Yocom, K. P. (2019). Reintegrating the North American

    beaver (*Castor canadensis*) in the urban landscape. *Wiley Interdisciplinary Reviews:*

    Water, *6*(1), e1323. https://doi.org/10.1002/wat2.1323

Bhaskar, A. S., Beesley, L., Burns, M. J., Fletcher, T. D., Hamel, P., Oldham, C. E., Roy, A.

    H. (2016). Will it rise or will it fall? Managing the complex effects of urbanization on

    base flow. *Freshwater Science*, *35*(1), 293–310. https://doi.org/10.1086/685084

Botter, G., Bertuzzo, E., Rinaldo, A. (2010). Transport in the hydrologic response: Travel time

    distributions, soil moisture dynamics, and the old water paradox. *Water Resources*

    Research, *46*(3). https://doi.org/10.1029/2009WR008371

Botter, G., Bertuzzo, E., Rinaldo, A. (2011). Catchment residence and travel time

    distributions: The master equation. *Geophysical Research Letters*, *38*(11).

    https://doi.org/10.1029/2011GL047666

Brazier, R. E., Puttock, A., Graham, H. A., Auster, R. E., Davies, K. H., Brown, C. M. L.

(2021). Beaver: Nature's ecosystem engineers. *WIREs Water*, *8*(1).

https://doi.org/10.1002/wat2.1494

Daniel, C.C., White, R.K., Stone, P.A. (1989). Ground water in the Piedmont. *Clemson University,* 336-338.

Diem, J. E., Hill, T. C., Milligan, R. A. (2018). Diverse multi-decadal changes in streamflow within a rapidly urbanizing region. *Journal of Hydrology*, *556*, 61–71.

https://doi.org/10.1016/j.jhydrol.2017.10.026

Drummond, J. D., Covino, T. P., Aubeneau, A. F., Leong, D., Patil, S., Schumer, R., Packman, A. I. (2012). Effects of solute breakthrough curve tail truncation on residence time estimates: A synthesis of solute tracer injection studies. *Journal of Geophysical Research: Biogeosciences*, *117*(G3), n/a-n/a. https://doi.org/10.1029/2012JG002019

Environmental Protection Agency. (2009). *Stormwater Wet Pond and Wetland Management Guidebook*. Retrieved from https://www3.epa.gov/npdes/pubs/pondmgmtguide.pdf

Fiori, A., and D. Russo (2008), Travel time distribution in a hillslope: Insight from numerical simulations, *Water Resources Research*, *44*(12), doi:W1242610.1029/2008wr007135.

Gaullier, C., Dousset, S., Baran, N., Kitzinger, G., Coureau, C. (2020). Influence of hydrodynamics on the water pathway and spatial distribution of pesticide and metabolite concentrations in constructed wetlands. *Journal of Environmental Management*, *270*, 110690. https://doi.org/10.1016/j.jenvman.2020.110690

Gaullier, C., Baran, N., Dousset, S., Devau, N., Billet, D., Kitzinger, G., Coisy, E. (2019). Wetland hydrodynamics and mitigation of pesticides and their metabolites at pilot-scale. *Ecological Engineering*, *136*, 185–192. https://doi.org/10.1016/j.ecoleng.2019.06.019

Golden, H. E., Hoghooghi, N. (2018). Green infrastructure and its catchment-scale effects: An

emerging science: Green infrastructure and its catchment-scale effects. *Wiley Interdisciplinary Reviews: Water*, *5*(1), e1254. https://doi.org/10.1002/wat2.1254

Graham, H. A., Puttock, A. K., Elliott, M., Anderson, K., Brazier, R. E. (2022). Exploring the dynamics of flow attenuation at a beaver dam sequence. *Hydrological Processes*, *36*(11), e14735. https://doi.org/10.1002/hyp.14735

Harman, C.J., Ward, A.S., Ball, A. (2016). How does reach-scale stream-hyporheic transport vary with discharge? Insights from rSAS analysis of sequential tracer injections in a headwater mountain stream. *Water Resources Research,* 52, 7130-7150. doi:10.1002/2016WR018832.

Harman, C.J. (2015). Time-variable transit time distributions and transport: Theory and application to storage-dependent transport of chloride in a watershed. *Water Resources Research,* 51, 1-30. doi:10.1002/2014WR015707.

Headley, T. R., Kadlec, R. H. (2007). Conducting hydraulic tracer studies of constructed wetlands: A practical guide. *Ecohydrology & Hydrobiology*, *7*(3–4), 269–282. https://doi.org/10.1016/S1642-3593(07)70110-6

Heidbüchel, I., Troch, P. A., Lyon, S. W., Weiler, M. (2012). The master transit time distribution of variable flow systems. *Water Resources Research*, *48*(6). https://doi.org/10.1029/2011WR011293

Higgins, M.W., Crawford, T.J., Atkins, R.L., Crawford, R.F. (2003). Geologic map of the Atlanta 30' x 60' quadrangle, Georgia. *U.S. Geological Survey,* Geologic Investigations Series Map 1-2602.

Holland, J. F., Martin, J. F., Granata, T., Bouchard, V., Quigley, M., Brown, L. (2004). Effects of wetland depth and flow rate on residence time distribution characteristics. *Ecological*

Engineering, *23*(3), 189–203. https://doi.org/10.1016/j.ecoleng.2004.09.003

Hrachowitz, M., Benettin, P., van Breukelen, B. M., Fovet, O., Howden, N. J. K., Ruiz, L., van der Velde, Y., Wade, A. J. (2016). Transit times-the link between hydrology and water quality at the catchment scale: Linking hydrology and transit times. *Wiley Interdisciplinary Reviews: Water*, *3*(5), 629–657. https://doi.org/10.1002/wat2.1155

Kadlec, R. H. (1994). Detention and mixing in free water wetlands. *Ecological Engineering*, *3*(4), 345–380. https://doi.org/10.1016/0925-8574(94)00007-7

Kaplan, D., Bachelin, M., Yu, C., Muñoz-Carpena, R., Potter, T. L., Rodriguez-Chacón, W. (2015). A hydrologic tracer study in a small, natural wetland in the humid tropics of Costa Rica. *Wetlands Ecology and Management*, *23*(2), 167–182. https://doi.org/10.1007/s11273-014-9367-1

Kaushal, S. S., Belt, K. T. (2012). The urban watershed continuum: Evolving spatial and temporal dimensions. *Urban Ecosystems*, *15*(2), 409–435. https://doi.org/10.1007/s11252-012-0226-7

Kilpatrick, F.A., Cobb, E.D., 1985, Measurement of discharge using tracers: U.S. Geological Survey Techniques of Water-Resources Investigations, book 3, chap. A16, 52 p.

Kim, M., L. A. Pangle, C. Cardoso, M. Lora, T. H. M. Volkmann, Y. Wang, C. J. Harman, P. A. Troch (2016), Transit time distributions and StorAge Selection functions in a sloping soil lysimeter with time-varying flow paths: Direct observation of internal and external transport variability, *Water Resources Research*, *52*(9), 7105-7129, doi:10.1002/2016WR018620.

Kusin, F. M., Jarvis, A. P., Gandy, C. J. (2014). Hydraulic Performance and Iron Removal in Wetlands and Lagoons Treating Ferruginous Coal Mine Waters. *Wetlands*, *34*(3), 555–

564. https://doi.org/10.1007/s13157-014-0523-4

Laurent, J., Bois, P., Nuel, M., Wanko, A. (2015). Systemic models of full-scale Surface Flow

Treatment Wetlands: Determination by application of fluorescent tracers. *Chemical*

Engineering Journal, *264*, 389–398. https://doi.org/10.1016/j.cej.2014.11.073

Lazar, J. G., Addy, K., Gold, A. J., Groffman, P. M., McKinney, R. A., Kellogg, D. Q. (2015).

Beaver Ponds: Resurgent Nitrogen Sinks for Rural Watersheds in the Northeastern

United States. *Journal of Environmental Quality*, *44*(5), 1684–1693.

https://doi.org/10.2134/jeq2014.12.0540

LeGrand, H.E. (1967). Ground Water of the Piedmont and Blue Ridge Provinces in the

Southeastern States. *Geological Survey Circular,* 538. 10.3133/cir538

Lewis, S., Nir, A. (1978). On tracer theory in geophysical systems in the steady and non-

steady state Part II. Non-steady state-theoretical introduction. *Tellus*, *30*(3), 260–271.

https://doi.org/10.1111/j.2153-3490.1978.tb00841.x

Mallin, M. A., Ensign, S. H., Wheeler, T. L., Mayes, D. B. (2002). Pollutant Removal

Efficacy of Three Wet Detention Ponds. *Journal of Environmental Quality*, *31*(2), 654–

660. https://doi.org/10.2134/jeq2002.6540

Moore, M. F., Vasconcelos, J. G., Zech, W. C., Soares, E. P. (2016). A procedure for

resolving thermal artifacts in pressure transducers. *Flow Measurement and*

Instrumentation, *52*, 219–226. https://doi.org/10.1016/j.flowmeasinst.2016.10.010

Morales, K., Oswald, C. (2020). Water age in stormwater management ponds and stormwater

management pond-treated catchments. Hydrological Processes, 34(8), 1854–1867.

https://doi.org/10.1002/hyp.13697

Miles, B., Band, L. E. (2015). Green infrastructure stormwater management at the watershed

scale: Urban variable source area and watershed capacitance. *Hydrological Processes*, *29*(9), 2268–2274. https://doi.org/10.1002/hyp.10448

Miller, A.J., Welty, C., Duncan, J.M., Baeck, M.L., Smith, J.A. (2021). Assessing urban rainfall-runoff response to stormwater management extent. *Hydrological Processes,* e14287. https://doi.org/10.1002/hyp.14287

National Weather Service. (2022). Climate NOWData. *National Oceanic and Atmospheric Administration.* https://www.weather.gov/wrh/Climate?wfo=ffc

Naiman, R. J., Johnston, C. A., Kelley, J. C. (1988). Alteration of North American Streams by Beaver. *BioScience*, *38*(11), 753–762. https://doi.org/10.2307/1310784

Neumayer, M., Teschemacher, S., Schloemer, S., Zahner, V., Rieger, W. (2020). Hydraulic Modeling of Beaver Dams and Evaluation of Their Impacts on Flood Events. *Water*, *12*(1), 300. https://doi.org/10.3390/w12010300

Niemi, A. J. (1977), Residence Time Distributions of Variable Flow Processes. *International Journal of Applied Radiation and Isotopes*, *28*(10-1), 855-860, doi:10.1016/0020-708x(77)90026-6.

Nuel, M., Laurent, J., Bois, P., Heintz, D., Mosé, R., Wanko, A. (2017). Seasonal and ageing effects on SFTW hydrodynamics study by full-scale tracer experiments and dynamic time warping algorithms. *Chemical Engineering Journal*, *321*, 86–96. https://doi.org/10.1016/j.cej.2017.03.013

Nyssen, J., Pontzeele, J., Billi, P. (2011). Effect of beaver dams on the hydrology of small mountain streams: Example from the Chevral in the Ourthe Orientale basin, Ardennes, Belgium. *Journal of Hydrology*, *402*(1–2), 92–102. https://doi.org/10.1016/j.jhydrol.2011.03.008

O'Driscoll, M., Clinton, S., Jefferson, A., Manda, A., McMillan, S. (2010). Urbanization

    Effects on Watershed Hydrology and In-Stream Processes in the Southern United States.

    Water, *2*(3), 605–648. https://doi.org/10.3390/w2030605

Paul, M. J., Meyer, J. L. (2001). Streams in the Urban Landscape. *Annual Review of Ecology*

    and Systematics, *32*(1), 333–365.

    https://doi.org/10.1146/annurev.ecolsys.32.081501.114040

Persson, J., Wittgren, H. B. (2003). How hydrological and hydraulic conditions affect

    performance of ponds. *Ecological Engineering*, *21*(4–5), 259–269.

    https://doi.org/10.1016/j.ecoleng.2003.12.004

Pugliese, L., Kusk, M., Iversen, B. V., Kjaergaard, C. (2020). Internal hydraulics and wind

    effect in a surface flow constructed wetland receiving agricultural drainage water.

    Ecological Engineering, *144*, 105661. https://doi.org/10.1016/j.ecoleng.2019.105661

Puttock, A., Graham, H. A., Ashe, J., Luscombe, D. J., Brazier, R. E. (2021). Beaver dams

    attenuate flow: A multi-site study. *Hydrological Processes*, e14017.

    https://doi.org/10.1002/hyp.14017

Puttock, A., Graham, H. A., Cunliffe, A. M., Elliott, M., Brazier, R. E. (2017). Eurasian

    beaver activity increases water storage, attenuates flow and mitigates diffuse pollution

    from intensively-managed grasslands. *Science of The Total Environment*, *576*, 430–443.

    https://doi.org/10.1016/j.scitotenv.2016.10.122

Rinaldo, A., Beven, K. J., Bertuzzo, E., Nicotina, L., Davies, J., Fiori, A., Russo, D., Botter,

    G. (2011). Catchment travel time distributions and water flow in soils. *Water Resources*

    Research, *47*(7). https://doi.org/10.1029/2011WR010478

Schuetz, T., Weiler, M., Lange, J. (2012). Multitracer assessment of wetland succession:

Effects on conservative and nonconservative transport processes. *Water Resources Research*, *48*(6). https://doi.org/10.1029/2011WR011292

Soulsby, C., Birkel, C., Tetzlaff, D. (2014). Assessing urbanization impacts on catchment transit times. *Geophysical Research Letters*, *41*(2), 442–448. https://doi.org/10.1002/2013GL058716

Strassler, E., Pritts, J., Strellec, K. (1999). Preliminary Data Summary of Urban Storm Water Best Management Practices (Report No. EPA-821-R-99-012). U.S. Environmental Protection Agency. https://www.epa.gov/sites/production/files/2015-11/documents/urban-stormwater-bmps_preliminary-study_1999.pdf

Sun, Y., Li, Q., Liu, L., Xu, C., Liu, Z. (2014). Hydrological simulation approaches for BMPs and LID practices in highly urbanized area and development of hydrological performance indicator system. *Water Science and Engineering,* 7(2), 143-154. https://doi.org/10.3882/j.issn.1674-2370.2014.02.003.

Terando, A. J., Costanza, J., Belyea, C., Dunn, R. R., McKerrow, A., Collazo, J. A. (2014). The Southern Megalopolis: Using the Past to Predict the Future of Urban Sprawl in the Southeast U.S. *PLoS ONE*, *9*(7), e102261. https://doi.org/10.1371/journal.pone.0102261

Van Der Velde, Y., Torfs, P., Van Der Zee, S., Uijlenhoet, R. (2012). Quantifying catchment-scale mixing and its effect on time-varying travel time distributions. *Water Resources Research*, 48, W06536. https://doi.org/10.1029/2011WR011310

Van Metre, P. C., Waite, I. R., Qi, S., Mahler, B., Terando, A., Wieczorek, M., Meador, M., Bradley, P., Journey, C., Schmidt, T., Carlisle, D. (2019). Projected urban growth in the southeastern USA puts small streams at risk. *PLOS ONE*, *14*(10), e0222714. https://doi.org/10.1371/journal.pone.0222714

Walsh, C. J., Roy, A. H., Feminella, J. W., Cottingham, P. D., Groffman, P. M., Morgan, R. P.
(2005). The urban stream syndrome: Current knowledge and the search for a cure.
Journal of the North American Benthological Society, 24(3), 706–723.
https://doi.org/10.1899/04-028.1

Wang, X., Shaw, E. L., Westbrook, C. J., Bedard-Haughn, A. (2018). Beaver dams induce
hyporheic and biogeochemical changes in riparian areas in a mountain peatland.
Wetlands, *38*(5), 1017–1032. https://doi.org/10.1007/s13157-018-1059-9

Weiss, P. T., Gulliver, J. S., Erickson, A. J. (2007). Cost and pollutant removal of storm-water
treatment practices. *Journal of Water Resources Planning and Management.* 133(3).
https://doi.org/10.1061/(ASCE)0733-9496(2007)133:3(218)

Wegener, P., Covino, T., Wohl, E. (2017). Beaver-mediated lateral hydrologic connectivity,
fluvial carbon and nutrient flux, and aquatic ecosystem metabolism. *Water Resources
Research*, *53*(6), 4606–4623. https://doi.org/10.1002/2016WR019790

Westbrook, C. J., Ronnquist, A., Bedard-Haughn, A. (2020). Hydrological functioning of a
beaver dam sequence and regional dam persistence during an extreme rainstorm.
Hydrological Processes, *34*(18), 3726–3737. https://doi.org/10.1002/hyp.13828

Whitmer, S., Baker, L., Wass, R. (2000). Loss of Bromide in a Wetland Tracer Experiment.
Journal of Environmental Quality, *29*(6), 2043–2045.
https://doi.org/10.2134/jeq2000.00472425002900060043x

Zarnetske, J. P., Haggerty, R., Wondzell, S. M., Baker, M. A. (2011). Dynamics of nitrate
production and removal as a function of residence time in the hyporheic zone. Journal of
Geophysical Research-Biogeosciences, 116, G01025.
https://doi.org/10.1029/2010JG001356

APPENDICES

Appendix A: Site Geochemical Parameters

Site	Location	Mean pH	Mean Specific Conductivity (uS/cm)	Mean Dissolved Oxygen (mg/L)
BH	In	6.9 ± 0.2	212.8 ± 63.0	9.7 ± 2.8
BH	Out	6.8 ± 0.2	206.2 ± 59.1	9.4 ± 2.8
CP	In	6.4 ± 0.2	197.8 ± 43.7	7.3 ± 4.5
CP	Out	6.7 ± 0.2	204.7 ± 49.4	7.9 ± 3.4
SC	In	6.7 ± 0.2	72.7 ± 20.7	8.2 ± 2.2
SC	Out	6.4 ± 0.4	94.2 ± 26.9	8.4 ± 7.1
MC	In	6.7 ± 0.2	155.9 ± 35.3	10.2 ± 3.2
MC	Out	7.2 ± 0.5	110.7 ± 29.9	10.6 ± 3.8
GA400	In	7.4 ± 0.3	215.7 ± 46.2	11.3 ± 3.4
GA400	Out	7.1 ± 0.3	173.4 ± 40.2	10.1 ± 9.4

Site	Location	Mean Fl (mg/L)	Mean Cl (mg/L)	Mean NO3 (mg N/L)	Mean SO4 (mg/L)	Mean Na (mg/L)	Mean K (mg/L)	Mean Mg (mg/L)	Mean Ca (mg/L)
BH	In	0.09 ± 0.03	15.3 ± 12.8	0.61 ± 0.18	10.7 ± 2.9	12.4 ± 10.4	3.7 ± 0.7	3.6 ± 1.2	17.6 ± 4.5
BH	Out	0.09 ± 0.03	14.3 ± 11.5	0.61 ± 0.18	9.8 ± 2.7	11.6 ± 9.3	3.7 ± 0.6	3.3 ± 1.1	16.6 ± 4.3
CP	In	0.07 ± 0.05	12.7 ± 4.3	1.41 ± 0.94	9.0 ± 3.1	10.0 ± 4.2	3.9 ± 1.3	3.7 ± 1.3	14.9 ± 4.7
CP	Out	0.06 ± 0.02	12.8 ± 4.2	1.03 ± 0.52	9.6 ± 2.3	10.5 ± 3.5	3.4 ± 0.5	4.1 ± 1.0	16.7 ± 4.2
SC	In	0.04 ± 0.01	3.9 ± 0.8	0.08 ± 0.10	1.2 ± 0.6	3.5 ± 0.8	2.1 ± 0.4	1.5 ± 0.2	4.2 ± 0.6
SC	Out	0.06 ± 0.02	4.3 ± 0.8	0.22 ± 0.10	1.8 ± 0.5	3.7 ± 0.7	2.2 ± 0.4	1.8 ± 0.3	6.4 ± 1.1
MC	In	0.06 ± 0.04	9.6 ± 4.6	0.60 ± 0.16	5.4 ± 1.0	10.5 ± 3.9	2.5 ± 0.3	2.2 ± 0.5	11.9 ± 2.3
MC	Out	0.07 ± 0.03	5.5 ± 1.7	0.18 ± 0.16	3.4 ± 3.1	5.9 ± 2.0	2.4 ± 0.3	1.4 ± 0.4	8.4 ± 1.8
GA400	In	0.06 ± 0.04	14.4 ± 2.5	1.48 ± 0.41	14.7 ± 2.7	13.0 ± 2.6	3.1 ± 0.5	2.8 ± 0.5	19.4 ± 3.3
GA400	Out	0.20 ± 0.06	10.5 ± 4.9	0.28 ± 0.16	8.6 ± 2.2	10.7 ± 4.4	2.9 ± 0.4	2.1 ± 0.4	14.6 ± 2.6